Journal of Biomedical Optics

SPIEDigitalLibrary.org/jbo

Ultrasensitive opto-microfluidic immunosensor integrating gold nanoparticle–enhanced chemiluminescence and highly stable organic photodetector

Nuno Miguel Matos Pires
Tao Dong

SPIE

Ultrasensitive opto-microfluidic immunosensor integrating gold nanoparticle–enhanced chemiluminescence and highly stable organic photodetector

Nuno Miguel Matos Pires and Tao Dong*
Buskerud and Vestfold University College, Department of Micro and Nano Systems Technology, Faculty of Technology and Maritime Sciences, P.O. 2243, N-3103 Tonsberg, Norway

Abstract. The expensive fabrication of current opto-microfluidic sensors is a barrier to the successful adoption of these devices in point-of-care testing. This work reports a simple inexpensive opto-microfluidic device incorporating a poly(dimethylsiloxane)-glass hybrid microfluidic chip modified with gold nanoparticles and a high-detectivity, high-stability organic photodetector. The enhancing effect of the gold nanoparticles on horseradish peroxidase-luminol-H_2O_2 chemiluminescence was exploited in rapid single-analyte immunoassays. The limit of detection for 17-β estradiol was 2.5 pg/ml, which is ~200 times more sensitive than previously reported chemiluminescent immunosensors employing other organic photodetectors. Detection was also demonstrated in complex media, including natural water and blood serum. © *2014 Society of Photo-Optical Instrumentation Engineers (SPIE)* [DOI: 10.1117/1.JBO.19.3.030504]

Keywords: integrated microfluidics; gold nanoparticles; chemiluminescent immunoassay; organic photodiode; cancer diagnostics.

Paper 130919LRR received Dec. 31, 2013; revised manuscript received Feb. 5, 2014; accepted for publication Feb. 5, 2014; published online Mar. 10, 2014.

Microfluidic optical devices are particularly suited for point-of-care analyte testing (POCT), and recent works[1,2] have acknowledged their potential role in cancer diagnostics, public health, and environment protection. To achieve POCT, simplicity, low cost, and portability are essential. Among various optical assays, the chemiluminescence (CL) immunoassay is a simple but ideal solution for POCT, which is based on specific antibody–antigen interaction coupled with horseradish peroxidase (HRP)-luminol-H_2O_2 luminescent reaction. A microfluidic CL detection system eliminates the need for external focusing optics and excitation sources,[3] unlike a fluorescence-based system.[4] In CL immunoassays, emitted 425- to 450-nm light is conventionally detected as either current or voltage using off-chip charge-coupled devices, photomultiplier tubes, or on-chip silicon photodiodes. While off-chip sensors are difficult to miniaturize into portable devices,[3] on-chip silicon detectors involve complex microfabrication, which restrains their use in inexpensive microfluidic systems.[5] On the contrary, organic photodetectors (OPDs) can be fabricated at low cost by simple spin-coating or spray-coating. The advantage of realizing thin device architectures (<1 μm) onto glass or plastic substrates makes OPDs well suited for integrated opto-microfluidics. Thus, the combination of OPDs with microfluidic CL immunoassays holds promise for truly disposable and compact devices.

Biosensor sensitivity is also of particular concern in POCT systems. However, the OPDs recently reported for integrated microfluidic systems[6] are still inferior to their silicon counterparts in optoelectronic performance. Bulk heterojunction OPDs based on blends of poly(3-hexylthiophene) (P3HT) and [6, 6]-phenyl-C_{61}-butyric acid methyl ester ($PC_{60}BM$) (Ref. 5) typically show specific detectivities (D^*) of $<10^{11}$ Jones, while the typical D^* of Si photodetectors are $\sim 4 \times 10^{12}$ Jones.[7] The development of OPDs of improved detectivity is essential to realize integrated microfluidic devices of high sensitivity. Nevertheless, the sensitivity can also be improved by the enhancement of the CL-based detection. Gold nanoparticles (AuNPs) can act as an enhancer of HRP-luminol-H_2O_2 CL reactions[8] besides their use in surface plasmon resonance or fluorescence spectroscopy. The enhancing effect of AuNPs could be applied to immunoassays while keeping the simplicity of the assay procedure. Despite this, AuNPs-based CL immunoassays have not yet been exploited in opto-microfluidic devices.

This work reports on the development of an integrated opto-microfluidic device to perform enhanced CL immunoassays using AuNPs and high-detectivity OPD. The motivation here is to realize a miniaturized ultrasensitive approach for simple inexpensive POCT systems. The device integrates a glass slide with immobilized AuNPs to a poly(dimethylsiloxane) (PDMS) microchannel, fabricated by standard replica molding. The setup is completed by the attachment of a bulk heterojunction OPD based on poly[$N-9'$-heptadecanyl-2, 7-carbazole-alt-5, 5-($4', 7'$-di-2-thienyl-$2', 1', 3'$-benzothiadiazole)](PCDTBT):$PC_{70}BM$ blend, prepared by spin-coating on indium tin oxide (ITO)-coated glass slide. The integrated device was assembled via PDMS-glass bonding by use of simple oxygen plasma. Rapid microfluidic CL immunoassays were conducted in close proximity to immobilized AuNPs, and subsequent CL signals were detected as photocurrent by the OPD.

The integrated AuNP-CL device is shown in Fig. 1. The PDMS microchannel consisted of nine parallel channel segments connecting one inlet and one outlet. Each channel segment measured 280 μm in width and 80 μm in depth. Separated nanoparticle lines covered the channel segments, which were previously assembled on the cover glass using 280-μm-wide trenches patterned on an auxiliary PDMS layer [Fig. 1(a)]. A reversible bonding method was used for the auxiliary PDMS and cover glass, thus permitting easy demounting [Fig. 1(b)] of the parts before permanent attachment of the cover glass to the PDMS channel layer [Figs. 1(c) and 1(d)]. The area (4×4 mm^2) occupied by the AuNP lines on the glass matched to the active area of the integrated OPD. The procedure of AuNP immobilization included pretreatment of the AuNP surface and glass surface with dithiodipropionic acid and 3-aminopropyltriethoxysilane,

*Address all correspondence to: Tao Dong, E-mail: tao.dong@hbv.no

0091-3286/2014/$25.00 © 2014 SPIE

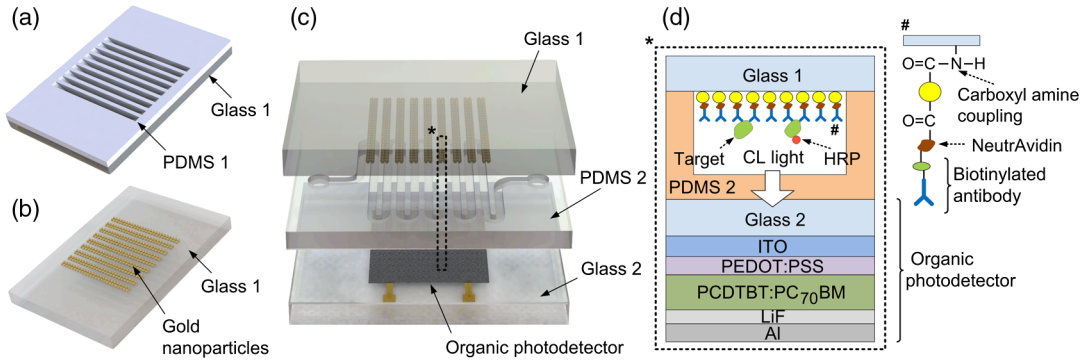

Fig. 1 Microfluidic gold nanoparticle (AuNP) optical immunosensor. PDMS, polydimethylsiloxane; CL, chemiluminescence; HRP, horseradish peroxidase. (a) Hybrid PDMS-glass chip with ~280 μm width microchannels for AuNP deposition. (b) Resultant glass slide with covalently bonded AuNP. (c) Microfluidic integration of AuNP glass slide, PDMS microchannel chip, and organic photodetector. (d) Detection zone including photodetector design and AuNP-enhanced CL competitive immunoassay. Device layers are not to scale.

respectively, followed by covalent binding via carboxylamine coupling reaction. Unreacted carboxyl groups on the AuNPs were further combined with biotinylated IgG antibody using NeutrAvidin. This method formed a large stable sensing surface within the microchannel, enabling efficient capture of antigen along multiple nanoparticle lines.

Detection of captured antigen is carried out employing a competitive binding immunoassay principle. The target competes with added target-HRP conjugate for binding to antibody-modified AuNPs [Fig. 1(d)]. After washing out of unbounded material, the luminol-H_2O_2 substrate interacts with HRP, which catalyzes the luminescent reaction. The intensity of generated blue light (~425 nm) is inversely proportional to the concentration of target analyte. For these assay conditions, it is expected that D^* of an OPD, which is commonly expressed by $D^* = (A\Delta f)^{1/2}R/i_n$, where A is the effective area of the OPD, Δf is the electrical bandwidth, R is the responsivity, and i_n is the noise current, is majorly limited by the shot noise from the dark current. Thus, D^* can simply be calculated from the measured photocurrent (J_{ph}) and dark current (J_d) following

$$D^* = \frac{R}{(2qJ_d)^{1/2}} = \frac{(J_{ph}/I_{light})}{(2qJ_d)^{1/2}}, \tag{1}$$

where I_{light} is the incident light intensity and q is the elementary charge constant (1.6×10^{-19}C).

The PCDTBT:$PC_{70}BM$ bulk heterojunction active layer was employed for the integrated OPD, which has incorporated spin-coated poly(3,4-ethylenedioxythiophene):polystyrene sulfonate (PEDOT:PSS) as the hole transport layer and thermally evaporated LiF/Al as the top electrode. The detector was realized applying the diode architecture ITO(100 nm)/PEDOT:PSS(40 nm)/PCDTBT:$PC_{70}BM$(120 nm)/LiF(0.8 to 1 nm)/Al(100 nm) whose fabrication was previously described.[9] No protective encapsulation was used here. PCDTBT is remarkably stable against oxidation due to its deep highest occupied molecular orbital level.[10] Furthermore, the high short-circuit photocurrent and low dark current of the PCDTBT:$PC_{70}BM$ photodiode result in high D^* [Eq. (1)]. At zero bias, the calculated D^* was 9.2×10^{11} Jones for the detector under light-emitting diode illumination at 428 nm peak wavelength with 0.22 mW/cm^2 light intensity. Nevertheless, an enhanced D^* leads to a reduced noise equivalent power (NEP) level as demonstrated by

$$\text{NEP} = \frac{(A\Delta f)^{1/2}}{D^*}, \tag{2}$$

and an improved NEP means an enhanced signal-to-background-current ratio (S/B).

The S/B ratio was determined for a number of AuNP-CL assay tests. For the assays, 17-β estradiol (E2), an important endocrine disrupting compound detected in various water samples, was used as a model target and spiked in phosphate-buffered saline (PBS). E2 may be carcinogenic to human epithelial cells.[11] The tests were conducted after the nonspecific binding sites within the microchannel were blocked with a commercial blocking buffer. OPD photocurrent was measured immediately after 5-min exposure to the luminol (pH 11.2) and H_2O_2 solution using a 236 Keithley source-measure unit. The photocurrent obtained with 0 ng/mL E2-HRP was defined as background for S/B determination. The S/B ratio varied with the size of the AuNPs [Fig. 2(a)]. The decreased response for the AuNPs with diameter <60 nm was due to absorption of CL emission by the Au surface plasmon resonance (SPR) phenomenon.[12] The wavelength of SPR related absorption red shifts with the increase of AuNP size. Furthermore, the active surface area of the nanoparticles decreases with increasing particle size, and this may explain the reduced S/B for 100-nm AuNPs. No significant change in the OPD response was observed for a microchannel containing both 60- and 10-nm AuNPs at similar concentration. The concentration of E2-HRP conjugate was also found to be related to enhanced S/B. The variation of E2-HRP concentration from 1 to 20 ng/ml has led to an ~45% increase in detector response [Fig. 2(b)], which has resulted from an increased CL emission intensity.

Figure 3 shows the calibration curve for E2 in PBS after device optimization. The curve was normalized by subtracting the measured photocurrent from that of the control sample containing only E2-HRP, and the resultant photocurrent variation (ΔS) was fitted to a three-parameter logarithm equation at best. On the basis of the logarithmic fit, the detection limit was 2.5 pg/ml, which contrasts with 70 pg/ml obtained by CL immunoassays employing no AuNPs [Fig. 3(a)]. Furthermore, the lowest limit of previously reported OPD-based CL detection using P3HT:$PC_{60}BM$ photodetectors was 500 pg/ml.[6] A run cycle of the AuNP-CL assay would take ~20 min, including sample incubation and CL signal detection. The stability of

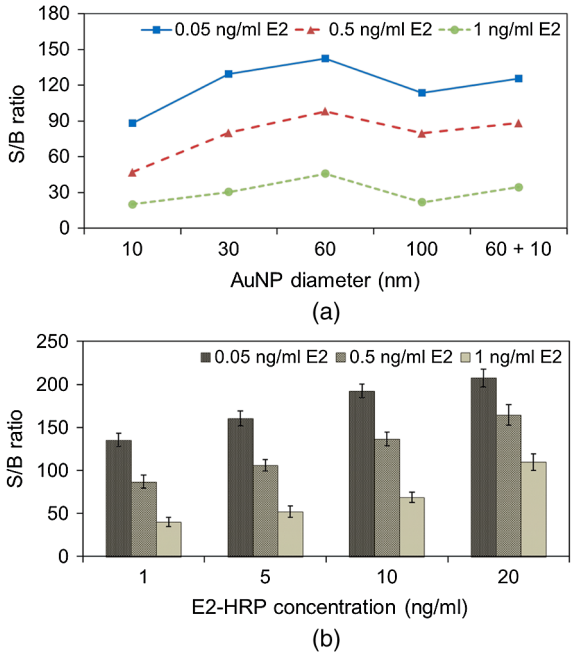

Fig. 2 Signal-to-background-current ratio (S/B) for the detection of 17-β estradiol (E2) in phosphate-buffered saline using the AuNP-enhanced CL competition immunoassay. (a) Effect of AuNP diameter on measured photocurrent. (b) Effect of varied E2-HRP conjugate concentrations. Error bar = standard deviation ($n = 3$).

the sensor response is relevant to single-use disposable POCT devices because of the possibility of long-term storage for these devices. The OPD-integrated AuNP-CL system was thus tested with 0.5 ng/ml E2 every three days and stored under ambient conditions between each test. After 15 days, the photocurrent

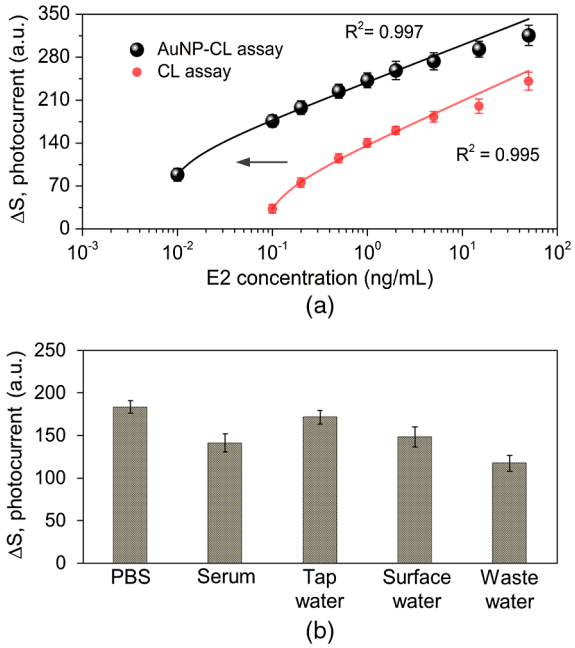

Fig. 3 Photocurrent variation (ΔS) due to different E2 concentrations. (a) Calibration plots obtained by performing CL assays and AuNP-enhanced CL assays. Arrow indicates decreased limit of detection. (b) E2 detection in different sample matrices. For ΔS determination, the measured photocurrent was subtracted from that obtained with the E2-HRP control. Error bar = standard deviation ($n = 3$).

response of one PCDTBT:$PC_{70}BM$ OPD decreased by only 25% of its initial value, presumably due to a small decrease in the charge mobilities of PCDTBT.[10] The integrated device was further challenged with human blood serum and real water samples. Water was spiked with 0.1 ng/ml E2 after sample filtration through 0.22-μm pore size filters, while serum contained 0.1 ng/ml E2 as detected by a conventional enzyme-linked immunosorbent assay. The results of ΔS shown in Fig. 3(b) indicated slight interferences from serum, surface water and wastewater effluent samples in the assays, which did not compromise the feasibility of E2 detection.

The enhancement of CL light intensity in proximity to AuNP lines, the high detectivity, and stability of the PCDTBT:$PC_{70}BM$ OPD and the possibility of detection in various complex matrices make the integrated device very promising for POCT. Ultrasensitivity was accompanied by rapid assay development and low-cost device fabrication. Moreover, the device concept can be broadly applied to other medically and environmentally relevant analytes.

Acknowledgments

Research is supported by Oslofjorfondet (regional kvalifiseringsstøtte, proj. no: 229857) and Research Council of Norway via long term support to NorFab (197411/V30). The authors acknowledge Nanjing University of S&T, XMU, and CAS Institute of Hydrobiology, in China, for the assistance to the experiments. We also thank Professors Nils Høivik, Ulrik Hanke for useful discussions.

References

1. J. Ozhikandathil and M. Packirisamy, "Silica-on-silicon waveguide integrated polydimethylsiloxane lab-on-a-chip for quantum dot fluorescence bio-detection," *J. Biomed. Opt.* **17**(1), 017006 (2012).
2. X. Zhao and T. Dong, "Multifunctional sample preparation kit and on-chip quantitative nucleic acid sequence-based amplification tests for microbial detection," *Anal. Chem.* **84**(20), 8541–8548 (2012).
3. J. R. Wojciechowski et al., "Organic photodiodes for biosensors miniaturization," *Anal. Chem.* **81**(9), 3455–3461 (2009).
4. N. M. M. Pires and T. Dong, "A cascade-like silicon filter for improved recovery of oocysts from environmental waters," *Environ. Technol.* **35**(6), 781–790 (2014).
5. V. Charwat et al., "Standardization of microfluidic cell cultures using integrated organic photodiodes and electrode arrays," *Lab Chip* **13**(5), 785–797 (2013).
6. R. Ishimatsu et al., "An organic thin film photodiode as a portable photodetector for the detection of alkylphenol polyethoxylates by a flow fluorescence-immunoassay on magnetic microbeads in a microchannel," *Talanta* **117**, 139–145 (2013).
7. X. Gong et al., "High-detectivity polymer photodetectors with spectral response from 300 nm to 1450 nm," *Science* **325**(5948), 1665–1667 (2009).
8. M. Yang et al., "Gold nanoparticle-based enhanced chemiluminescence immunosensor for detection of Straphylococcal Enterotoxin B (SEB) in food," *Int. J. Food Microbiol.* **133**(3), 265–271 (2009).
9. N. M. M. Pires et al., "Integrated optical microfluidic biosensor using a polycarbazole photodetector for point-of-care detection of hormonal compounds," *J. Biomed. Opt.* **18**(9), 097001 (2013).
10. A. J. Heeger, "Semiconducting polymers: the third generation," *Chem. Soc. Rev.* **39**(7), 2354–2371 (2010).
11. S. Yu et al., "17-Beta-estradiol induces neoplastic transformation in prostatic epithelial cells," *Cancer Lett.* **304**(1), 8–20 (2011).
12. G. Lu et al., "Influence of the nanoscale structure of gold thin films upon peroxidase-induced chemiluminescence," *App. Phys. Lett.* **88**(2), 023903 (2006).